RSC Advances

COMMUNICATION

View Article Online
View Journal | View Issue

Cite this: *RSC Adv.*, 2015, **5**, 24712

Received 1st December 2014
Accepted 19th February 2015

DOI: 10.1039/c4ra15602a

www.rsc.org/advances

Low-cost & low-temperature curable solution-processed silica-based nanostructured antireflective coatings on $CuIn_{1-x}Ga_xSe_2$ thin film solar cells†

Seung-Yeol Han,[abc] Changqing Pan,[ab] Dae-Hwan Kim[abd] and Chih-hung Chang*[abc]

A simple, low-cost and low-temperature curable silica-based antireflective coating (ARC) deposited by a solution-based process has been investigated for Cu(In,Ga)Se_2 (CIGS) solar cells for the first time. Thin-layer nanostructured ARCs featuring 20–30 nm SiO_2 NPs were fabricated from a simple, low-cost chemical solution. The silica-based nanostructured ARCs were deposited on a glass substrate and on CIGS solar cells. The nanostructured ARCs on glass could increase the transmittance by 3.9%. The nanostructured ARCs could reduce the reflectance of CIGS solar cells by 4.96%. The nanostructured ARCs on CIGS solar cells resulted in an enhancement of solar energy conversion efficiency from 16.0% to 17.2%. These enhancements confirm the utility of these simple nanostructured ARCs as a cost-effective solution for photon management in thin film CIGS solar cells.

Introduction

Antireflective coatings (ARCs) generally consist of one or more layers of dielectric material in the form of a quarter wavelength (QW) thickness film that exhibits a wavelength sensitive reduction in reflection due to optical interference.[1] Kuo *et al.* recently created a seven-layer structure, which includes TiO_2 films and SiO_2 nanorods, using oblique-angle deposition at different angles, and achieved an extremely low reflectance for silicon solar cells.[2] The use of more than two layers of ARCs is costly for large area PV applications. Multilayered films require precision and multiple deposition steps can therefore be expensive, thus single-layer QW ARCs are more commonly used in low-cost, large area applications. Currently, several low-cost ARC approaches are being researched for solar cell applications. In 1960, Bernhard discovered a periodic array of sub-wavelength protrusions on the cornea of moths.[3] These so-called "moth-eye" structures work on the principle of a gradient index of refraction.[4–6] These gradient surfaces can be thought of as having a low net reflectance based on the destructive interference of an infinite series of reflections at each incremental change in refractive index. More recently, researchers have found that the structures do not need to be periodic, only that the stochastic structure yields features that are on the whole smaller than the wavelength of visible light.[7] Engineers have found a variety of ways to mimic moth-eye nanostructures using ARCs deposited by electron-beam lithography,[8] nanoimprint lithography,[9] plasma-enhanced chemical vapor deposition (PECVD) and interference lithography.[10,11] However, these technologies all require high-cost capital equipment which can be difficult to adapt to the large area formats required for solar cell and window glass applications. For example, Chen *et al.* reported broadband and quasi-omnidirectional ARCs using an aperiodic array of silicon nanotips formed by high-density electron cyclotron resonance plasma etching on single-crystal silicon.[12] These techniques are too costly for large area solar PV applications. Various antireflective coatings using MgF_2 have been studied and used for reducing the reflectance of the surface of silicon and thin film CIGS solar cells.[13–15] The fabrication of MgF_2 thin films is normally carried out by physical vapor deposition. Physical vapor deposition such as sputtering is well known to be inefficient in terms of energy and material utilization. Recently, a number of research groups have demonstrated the use of nanostructured ZnO in effective ARCs for solar cells.[16–19] Liu *et al.* reported the use of ZnO nanowires as an ARC on micropyramid silicon solar cells with a low reflectance of 3.2%.[16] Han *et al.* reported the growth of ZnO nanorod arrays on a textured silicon substrate using a continuous flow microreactor.[17] Hsieh *et al.* reported an effective approach for enhancing the photoelectric conversion of Cu(In,Ga)Se_2 solar cells with three-dimensional ZnO

[a]*School of Chemical, Biological & Environmental Engineering, Oregon State University, Corvallis, Oregon 97331, USA. E-mail: changch@che.orst.edu*

[b]*Oregon Process Innovation Center, Microproducts Breakthrough Institute, Corvallis, Oregon 97330, USA*

[c]*CSD Nano, Inc., 720 NE Granger Ave. STE #B2, Corvallis, Oregon 97330, USA*

[d]*Green Energy Research Division, Daegu Gyeongbuk Institute of Science & Technology, Daegu, Korea*

† Electronic supplementary information (ESI) available. See DOI: 10.1039/c4ra15602a

nanotree arrays.[18] Jheng *et al.* reported the use of ZnO nanostructures as effective ARCs for Cu_2ZnSnS_4 (CZTS) thin film solar cells.[19] The nanostructured ZnO ARCs were fabricated using batch hydrothermal processes in the majority of these works. These batch processes require the immersion of entire solar cells into a bath, which is less desirable for manufacturing. Another promising low-cost approach has also been pursued by using silica nanoparticles and a dip-coating process to create single-layer QW porous silica ARCs on solar cover glasses.[20] This approach was actually developed by Moulton back in 1947.[21] More recently, DSM developed a single-layer inverse porous silica ARC technology, KepriCoat™. The inverse porous silica layer was created from polymer–silica core–shell particles.[22] The inverse porous structure lowers the surface roughness and increases the scratch resistance, durability, and cleanability. The core–shell particles were synthesized by coating a layer of silica nanoparticles on a spherical cationic polymer template. For example, a cationic polymer particle with a diameter of around 80 nm was used as a template. Tetramethyl orthosilicate was added to the polymer solution to form core–shell particles. The reaction was stopped by dilution with alcohol, followed by subsequent acidification with nitric acid. The core–shell particles were then mixed with inorganic silica binders to form a coating dispersion. The coatings were applied on both sides of the substrate by dip coating. The pores were then generated by removing the polymer particles during the tempering step.

In this study, a simple, low-cost and low-temperature curable AR coating solution was introduced, and the effectiveness of this nanostructured ARC for CIGS solar cells and for bare glass substrate was demonstrated.

Experimental

The deposition of antireflective coating was carried out on the surfaces of bare glass substrates and functional $CuIn_{1-x}Ga_xSe$ thin film solar cells. Functional $CuIn_{1-x}Ga_xSe_2$ (CIGS) solar cells and films were fabricated at the Daegu Gyeongbuk Institute of Science and Technology (DGIST). CIGS thin films were grown on soda-lime glass substrates with a 60 nm-thick coating of Mo through a three-stage process involving the co-evaporation of Cu, In, Ga, and Se. The three-stage process has been described in detail.[23] In the first step, an $(In,Ga)_2Se_3$ precursor was deposited on the substrate for 1500 seconds at 420 °C. In the second step, the Cu-rich CIGS films were grown with Cu and Se fluxes at 550 °C. In the third step, a small amount of In and Ga was evaporated to convert the Cu-rich CIGS films to Cu-poor CIGS films. The Se beam flux was kept constant throughout the deposition process, while the rate of Ga evaporation was varied. An average thickness of 2 μm was obtained for the CIGS films. A CdS buffer layer was deposited on the CIGS films by using a chemical bath deposition (CBD) method. The CdS thin film was deposited using an aqueous solution containing cadmium sulphate ($CdSO_4$), thiourea (CH_4N_2S) and ammonium hydroxide (NH_4OH). A 1 : 50 molar ratio of cadmium sulphate to thiourea was employed. The aqueous solution was maintained at 60 °C and deposited over 20 min. The deposited CdS thin film was annealed at 200 °C for 2 min on a hot plate, and a 60 nm-thick CdS thin film was obtained. Subsequently, 50 and 300 nm-thick i-ZnO and Al-doped ZnO (Al:ZnO) window layers were deposited by rf-sputtering. Finally, an Al electrode was deposited as the front contact by using a thermal evaporator.

MoreSun™, a sol–gel silica-based antireflective coating (ARC) solution, was supplied by CSD Nano, Inc. The silica nanoparticles (NPs) with sizes of 20–30 nm are well dispersed in an alcoholic solution. The glass substrates (3.2 mm Pilkington low iron glass) were cleaned with detergent and washed with DI water, acetone and isopropyl alcohol (IPA). The cleaned glass substrates were dried under air flow and kept in a dust-free container until the AR coating was applied. The AR coating solution was deposited on the bare glass substrates and on CIGS solar cells by spin coating. The thickness of the AR coating layer on the glass substrate was varied and optimized by changing the rotation speed, and then the optimized conditions for AR coating deposition were transferred to the surface of CIGS solar cells. The AR-coated CIGS cell samples were dried at 100 °C for 10 min in a vacuum oven to evaporate solvents and water. The optical properties, transmittance and reflectance of the AR-coated glass substrates and CIGS cells were studied using a UV-vis/NIR spectrophotometer (JASCO V-670) equipped with a 60 mm integrating sphere. The quantum efficiency (QE) of the solar cell was measured by using a real time quantum efficiency tester, Flash QE (Tau Science). The morphology and crystal structure of the CIGS films were measured by using scanning electron microscopy (SEM, Hitachi Co., S-4800), Atomic Force Microscopy (AFM, Vecco Innova SPM) and transmission electron microscopy (TEM, Hitachi Co., HF-3300). The electrical properties of the completed CIGS solar cells were investigated by using photocurrent (PC) spectroscopy and current–voltage (*I–V*) curves for a solar simulator at AM 1.5G illumination.

Results and discussion

To optimize the AR coating effect on the CIGS solar cells, MoreSun™, a sol–gel silica-based antireflective coating (ARC), was demonstrated on a glass substrate prior to application to the CIGS solar cells. The commercially available sol–gel silica-based AR coating solution (MoreSun™, CSD Nano, Inc., USA) provides a low-cost alternative to ARCs fabricated by vapor-phase techniques. The chemical solution has good long-term stability, with additional benefits for forming durable thin films *via* a low-temperature curing process. This solution can be applied by various solution coating processes, such as spin coating, dip coating, roll-to-roll slot die or gravure coating, and aerosol spray coating. A simple spin coating process was used on a single-sided glass substrate for this study. The single-sided AR-coated glass was cured on a hotplate at 100 °C for 10 min under ambient air. The cured nanostructured ARC showed good durability against a paper wipe test.

This level of scratch resistance was sufficient because the ARC layer on the CIGS cell would be covered underneath the EVA layer and the cover glass in a solar module assembly. More detailed mechanical and stability testing data for MoreSun™ coatings on solar cover glass are available from CSD Nano, Inc.

To evaluate the optical performance of the single-sided AR coating, transmittance measurements were carried out over the wavelength range of 300–1200 nm, which is the spectral response range of CIGS solar cells, as shown in Fig. 1. The most effective wavelength range of both solar radiation and CIGS spectral response is 400–750 nm, which is the range of the visible light spectrum. The sample deposited by the spin coating process was optimized to enhance the optical transmittance in this range, and it showed an average increase in transmittance of 3.9% over the wavelength range of 400–750 nm compared to that of bare glass substrate, as shown in Fig. 1b. The thickness of the ARC layer sample for optimized optical transmittance was investigated by SEM. As shown in Fig. S1,† a 130 nm-thick porous and well-packed uniform layer of silica NPs was formed. The thickness of 130 nm is well matched with the quarter wavelength of the peak transmittance at 510 nm. The AFM image and roughness profile are shown in Fig. S2a and b.† The silica-based nanostructured ARCs possess a nano-scale roughness with root mean square (RMS) = 2.92 nm as shown by the AFM analysis. The RMS indicates that the uniformity of the ARC layer is very smooth but that it has the nano-features of a moth-eye structure. The moth-eye mimic structure could be of additional benefit to enhance the reflection reduction. In order to investigate the structure on the top surface of the CIGS solar cells and the ARC layer, the AR coating on the surface of the CIGS solar cells could be observed by SEM, as shown in Fig. 2.

The clear contrast from the image shown in Fig. 2a could be attributed to the bumpy surface with a micro-scale roughness of the CIGS layer after a significant grain growth process. More

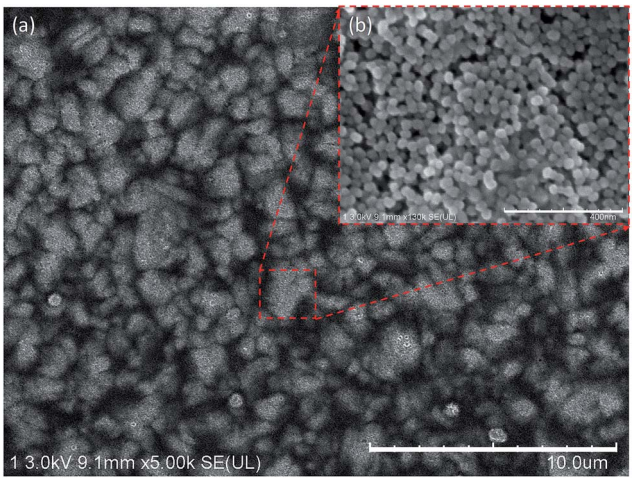

Fig. 2 Top-view SEM images of the AR coating on the surface of a CIGS solar cell: (a) low magnification (10 μm scale bar) and (b) high magnification (inset, 400 nm scale bar).

detailed structural characterization of the AR coating on the surface of the CIGS solar cell was carried out by cross-sectional TEM analysis, the results of which are given in Fig. 3.

The image shows a textured surface of Al-ZnO/i-ZnO/CdS films stacked on top of the large-grain, highly-crystalline CIGS absorbant layer with an average thickness of 2 μm.

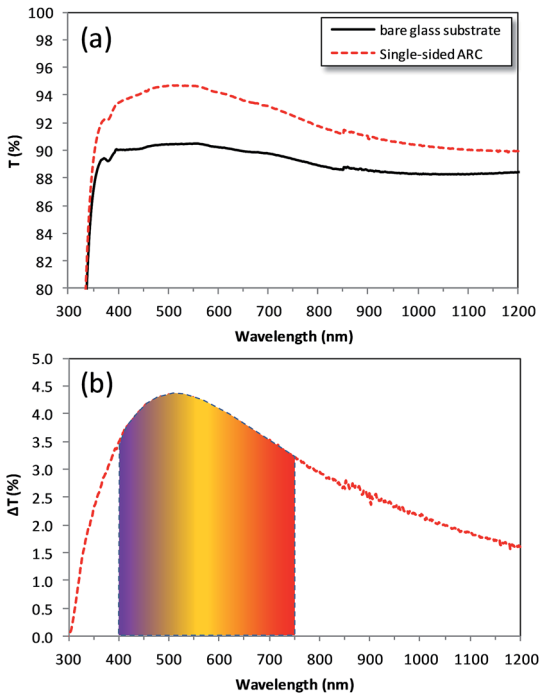

Fig. 1 (a) Optical transmittance of a single-sided AR coating layer deposited on a glass substrate and of the bare glass substrate; (b) enhancement of transmittance from the single-sided AR coating, ΔT.

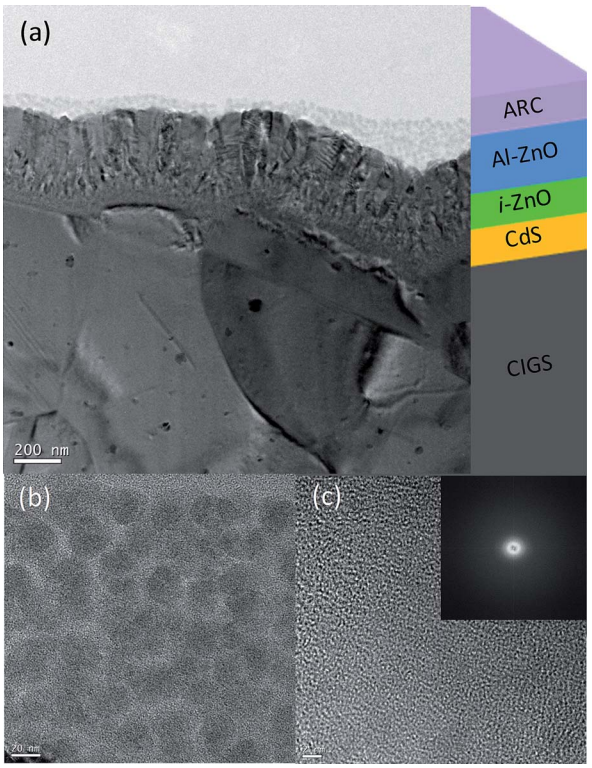

Fig. 3 TEM images of (a) cross-sectional CIGS solar cell with ARC layer, (b) silica NP AR coating layer (high resolution) and (c) silica NP (inset: diffraction pattern of silica NP).

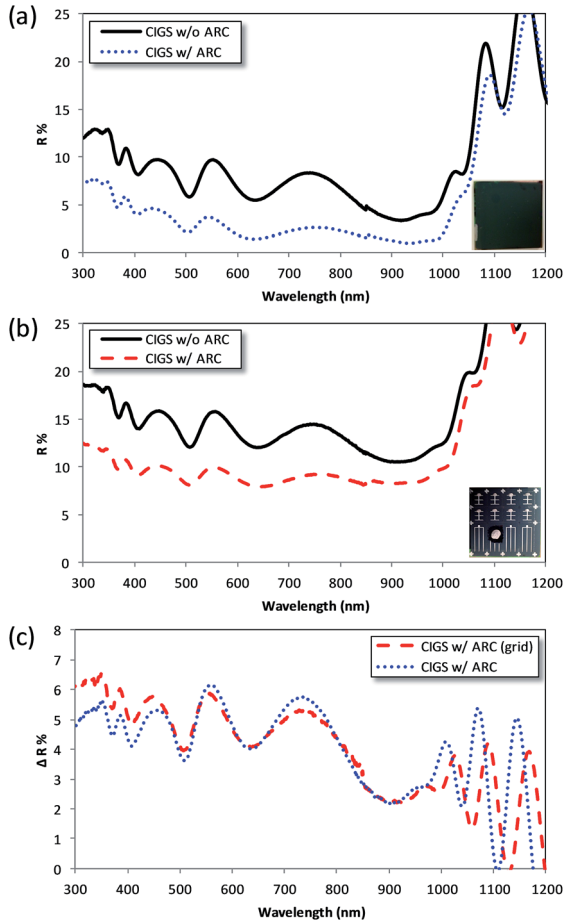

Fig. 4 Reflectance of (a) CIGS film with/without AR coating and (b) CIGS solar cell (w/ grid) with/without AR coating, and (c) enhancement, Δ*R*%, of the anti-reflectivity of the CIGS thin film and solar cell (w/ grid).

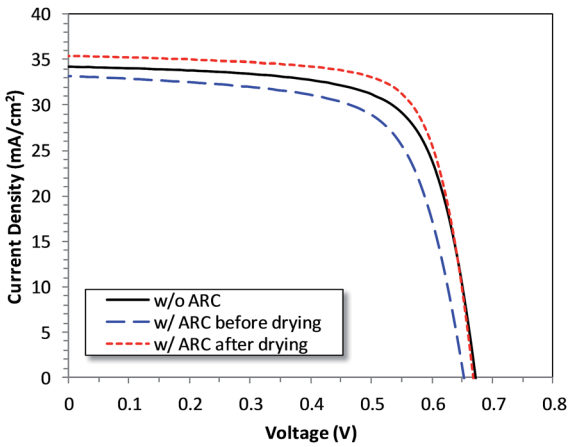

Fig. 5 *J*–*V* characteristics of CIGS solar cells with and without SiO_2 NP antireflective coatings.

A thin layer of silica NPs was observed on top of the CIGS solar cells. The thickness of the silica-based nanostructured ARC layer on the CIGS solar cells was not uniform due to the limitations of the spin coating process. The use of an optimized spray process should improve the uniformity. The nanostructured silica layer shows a porous structure, which leads to a low index of refraction because of air in the pores of the silica-based layer, as shown in Fig. 3a and b. However, given its microscale roughness, the textured surface of the CIGS solar cells was still retained, since the thickness of the silica layer was less than 200 nm, as shown in Fig. 2a and 3a. The SEM and TEM images given in Fig. 2b and 3b show a thin layer with high porosity, which consists of NPs with a uniform size of around 20–30 nm. The electron diffraction pattern taken from the silica-based nanostructured ARC layer shown in Fig. 3c indicates an amorphous structure.

To evaluate the optical performance of the antireflective coating on the CIGS solar cells, reflectance measurements with an integrating sphere were carried out over the UV-vis to near-IR spectral range, 300–1200 nm, as shown in Fig. 4. The average reflectance of the bare CIGS film with no grid was measured to be 7.70% in the visible wavelength range, 400–750 nm. After applying the silica-based nanostructured ARC on top of the CIGS solar cell, the average reflectance was significantly reduced to 2.80%, which corresponds to a 4.90% reduction in reflectance. CIGS solar cells (with grid, Al electrode) with/without AR coating showed much higher reflectances of 8.99% and 13.95%, respectively, because of reflection from the Al grids.

The reduction in reflectance was 4.96%, which is similar to the value of reduction for the CIGS cell without Al grids. A 4.0% reduction in reflectance was obtained for both samples over the UV-vis to near-IR wavelength range of 300–1200 nm. The reduction in reflectance of 4.96% over the UV-vis wavelength range is not the highest value for AR coatings on CIGS or other solar cells in view of previously published works.[14,15,18,24–26] For example, a MgF_2/SiN_x double-layer ARC has been used commercially for reducing the reflectance of the surface of silicon solar cells.[14,15] However, high-cost, low-throughput vacuum-based PVD and CVD are needed for the fabrication of these double-layer ARCs. Lower-cost, solution-based techniques have been explored for the fabrication of nanostructured ZnO ARCs for both silicon and thin film solar cells. Nanostructured ZnO antireflective coatings with a reduction in reflectance from 4.68–7.5% were demonstrated in these works.[18,24–26] However, the fabrication of these nanostructured ZnO AR coatings has mostly been performed by the immersion of entire solar cells within a batch hydrothermal reactor, which might pose some limitations for large scale manufacturing. In our previous work, a nanostructured ZnO ARC on textured silicon was demonstrated with a reduction in reflectance of up to 7.2% (ref. 17) by using a facile continuous solution process, which could resolve some of the issues of the batch hydrothermal reactor. The reduction in reflection from the silica-based nanostructured ARC deposited by spin coating is a comparable result with the one obtained from the hydrothermal approach. The current approach offers a simpler, cheaper and more scalable ARC solution than the batch hydrothermal technique. For example, the silica-based solution could be transferred to an aerosol-based spray coating process. The thickness of the silica-based

Table 1 Photovoltaic performance of CIGS solar cells with and without SiO_2 NP antireflective coatings

Sample	V_{oc} (V)	J_{sc} (mA cm^{-2})	FF (%)	Eff. η (%)	Improvement in η (%)
CIGS solar cell w/o ARC	0.67	34.2	69.8	16.0	—
CIGS solar cell w/ ARC, before drying	0.65	33.2	67.0	14.5	−1.5
CIGS solar cell w/ ARC, after drying	0.67	35.4	72.7	17.2	+1.2

AR coating layer on top of the CIGS solar cell as shown in Fig. 3a is not uniform because of the nature of spin coating. Spin coating is designed to spread a fluid to the edge of the substrate, leaving a thin film of fluid on a flat surface by centripetal acceleration. However, the top surface of the CIGS solar cell is not flat. The highly textured surface creates valleys for tapping more fluid, which results in a thicker film. It is believed that a more uniform silica-based AR coating on CIGS solar cells could further increase the reduction in reflection to more than 4.90%.

The CIGS solar cells were measured to evaluate the effect of the silica-based nanostructured ARC layer on the improvement in the external quantum efficiency (EQE), as shown in Fig. S3.† The CIGS solar cells with the silica-based nanostructured ARC show an excellent improvement in quantum efficiency of 4.60%, almost as much as the reduction in reflection of 4.90%.

The photovoltaic *J–V* characteristics were measured to evaluate the effect of the silica-based nanostructured ARC on the performance of CIGS solar cells, as plotted in Fig. 5, and the electrical parameters for all CIGS solar cells with/without the nanostructured ARC are summarized in Table 1. The performances of CIGS solar cells with the silica-based nanostructured ARC were also measured before and after drying the solar cells at 100 °C for 10 min.

The CIGS solar cell without AR coating achieved a conversion efficiency (η) as high as 16.0% with open-circuit voltage (V_{oc}) = 0.67 V, short-circuit current density (J_{sc}) = 34.2 mA cm^{-2}, and fill factor (FF) = 69.8%. The CIGS solar cells with the silica-based nanostructured ARC before and after the drying process showed solar energy conversion efficiencies (η) of 14.5% and 17.2%, with V_{oc} = 0.65 and 0.67 V, J_{sc} = 33.2 and 35.4 mA cm^{-2}, and FF = 67.0 and 72.7%, respectively. After applying the silica-based coating on the CIGS solar cell without drying, the performance of the CIGS solar cell decreased significantly because of the residue of solvent and moisture from the AR coating solution and the atmosphere. Olsen *et al.*[27] indicated that the dominant effect of moisture is a result of increased sheet resistance in the TCO layer. The effect of moisture ingress into the structure of thin film solar cells on J_{sc} and fill factor is significant. Therefore, J_{sc} decreases as a result of the increase in sheet resistance and series resistance, as does the fill factor. In Table 1, it can be seen that J_{sc} and the fill factor of the silica-based nanostructured ARC on the CIGS solar cell before drying decreased significantly compared to the CIGS solar cell without AR coating. As a result of the decreased J_{sc} and fill factor, the efficiency decreased from 16.0% to 14.5%. However, the benefits of the silica-based nanostructured ARC on the CIGS solar cell were demonstrated after removing the residual solvent and moisture from within the coated solar cell. The drying conditions of 100 °C for 10 min in a vacuum oven did not degrade the performance of the CIGS solar cells, which was proven by several performance tests using the same conditions. After drying the short circuit, J_{sc} of the CIGS solar cells with the nanostructured silica-based ARC increased significantly from 33.2 mA cm^{-2} to 35.4 mA cm^{-2}. The fill factor also increased from 67% to 72.7%. As a result of simply adding the low-cost, silica-based nanostructured ARC on top of the CIGS solar cell, J_{sc}, the fill factor and the solar energy conversion efficiency increased from 34.2 mA cm^{-2} to 35.4 mA cm^{-2}, 69.8% to 72.7% and 16.0% to 17.2%, respectively. The benefit of adding this simple and low-cost ARC layer on the CIGS solar cell is clearly seen from the 1.2% gain in energy conversion efficiency. It is believed that further improvement could be obtained from the nanostructured ARC after optimizing the film thickness and gradient of index of refraction *via* porosity control. The optimum thickness for maximizing the reduction in reflection would be roughly the quarter wavelength thickness, $\lambda/4$, with a single-layer coating. Appropriate solution-based deposition techniques are currently being explored to optimize the performance of silica-based nanostructured ARCs for CIGS solar cells.

Conclusions

A simple, low-cost and low-temperature curable silica-based nanostructured antireflective coating (ARC) deposited by a simple solution process was investigated for Cu(In,Ga)Se_2 (CIGS) thin film solar cells for the first time. The SEM and TEM characterization showed a porous silica layer that consists of NPs with a uniform size of around 20–30 nm. The electron diffraction pattern taken from the ARC layer indicated an amorphous structure. The obtained silica-based nanostructured ARC showed a significant reduction of reflection, resulting in more photons being brought into the solar cell. The silica-based ARC on bare glass substrate showed an increase in optical transmittance of 3.9%, and the AR coating on CIGS solar cells reduced the reflectance from 13.95% to 8.99%, which corresponds to a 4.96% reduction. This significant reduction of photon reflection within the UV-visible wavelength range resulted in more photons being brought into the CIGS solar cells. These additional photons increased the solar energy conversion efficiency value by 1.2%. This improvement is very attractive in view of its benefit for the cost ratio and ease of processing. Further studies are needed to transfer this low-cost solution into a CIGS module in terms of photon management. First of all, we will need to deposit our ARC on the cover glass.

Secondly, an investigation into adding an EVA layer on top of the AR coating on the CIGS layer will also need to be carried out.

Acknowledgements

The authors would like to acknowledge the financial support for this work from the DGIST R&D Programs of the Ministry of Education, Science and Technology of Korea (14-BD-05), NSF STTR phase II award IIP 1230456, and ONAMI GAP fund. The Flash QE was built and installed at the OPIC lab using an Oregon BEST equipment grant.

Notes and references

1 J. Zhao and M. A. Green, *IEEE Trans. Electron Devices*, 1991, **38**, 1925.
2 M.-L. Kuo, D. J. Poxson, Y. S. Kim, F. W. Mont, J. K. Kim, E. F. Schubert and S.-Y. Lin, *Opt. Lett.*, 2008, **33**, 2527.
3 C. G. Bernhard, *Endeavour*, 1967, **26**, 79.
4 P. B. Clapham and M. C. Hutley, *Nature*, 1973, **244**, 281.
5 K. Han and C.-h. Chang, *Nanomaterials*, 2014, **4**, 87–128.
6 S. A. Boden and D. M. Bagnall, *Progr. Photovolt.: Res. Appl.*, 2010, **18**, 195.
7 R. Leitel, J. Petschulat, A. Kaless, U. Schulz, O. Stenzel and N. Kaiser, *Proceedings of the SPIE*, 2005, **5965**, 534.
8 J.-Q. Xi, M. F. Schubert, J. K. Kim, E. F. Schubert, M. Chen, S.-Y. Lin, W. Liu and J. A. Smart, *Nat. Photonics*, 2007, **1**, 176.
9 J. Y. Chen and K. W. Sun, *Thin Solid Films*, 2011, **519**, 5194.
10 K.-C. Park, H. J. Choi, C.-H. Chang, R. E. Cohen, G. H. Mckinley and G. Barbastathis, *ACS Nano*, 2012, **6**, 3789.
11 S. L. Diedenhofen, G. Vecchi, R. E. Algra, A. Hartsuiker, O. L. Muskens, G. Immink, E. P. A. M. Bakkers, W. L. Vos and J. G. Rivas, *Adv. Mater.*, 2009, **21**, 973.
12 Y.-F. Huang, S. Chattopadhyay, Y.-H. Jen, C.-Y. Peng, T.-A. Liu, Y.-K. Hsu, C.-L. Pan, H.-C. Lo, C.-H. Hsu, Y.-H. Chang, C.-S. Lee, K.-H. Chen and L.-C. Chen, *Nat. Nanotechnol.*, 2007, **2**, 770.
13 I. Lee, D. G. Lim, S. H. Lee and J. Yi, *Surf. Coat. Technol.*, 2001, **137**, 86.
14 S. K. Dhungel, J. Yoo, K. Kim, S. Jung, S. Ghosh and J. Yi, *J. Korean Phys. Soc.*, 2006, **49**, 885.
15 J.-Y. Chu, M.-H. Chiueh, C.-T. Chen, Y.-P. Chen, M.-H. Wu and Y.-W. Tai, *J. Photonics Energy*, 2011, **1**, 017001.
16 Y. Liu, A. Das, S. Xu, Z. Lin, C. Xu, Z. L. Wang, A. Rohatgi and C. P. Wong, *Adv. Energy Mater.*, 2012, **2**, 47.
17 S.-Y. Han, B. K. Paul and C.-H. Chang, *J. Mater. Chem.*, 2012, **22**, 22906.
18 M.-Y. Hsieh, S.-Y. Kuo, H.-V. Han, J.-F. Yang, Y.-K. Liao, F.-I. Lai and H.-C. Kuo, *Nanoscale*, 2013, **5**, 3841.
19 B.-T. Jheng, P.-T. Liu and M.-C. Wu, *Sol. Energy Mater. Sol. Cells*, 2014, **128**, 275.
20 C. Balif, J. Dicker, D. Borchert and T. Hofmann, *Sol. Energy Mater. Sol. Cells*, 2004, **82**, 331.
21 H. R. Moulton, US 19470739544, US 19470405, 1947.
22 P. Buskens, N. Arfsten, R. Habets, H. Langermans, A. Overbeek, J. Scheerder, J. Thies and N. Viets, *Glass Performance Days 2009*, 2010, p. 505.
23 H.-J. Jo, D.-H. Kim, C. Kim, D.-K. Hwang, S.-J. Sung, J.-H. Kim and I.-H. Bae, *J. Korean Phys. Soc.*, 2012, **60**, 1708.
24 B.-K. Shin, T.-I. Lee, J. Xiong, C. Hwang, G. Noh, J.-H. Cho and J.-M. Myoung, *Sol. Energy Mater. Sol. Cells*, 2011, **95**, 2650.
25 B.-T. Jheng, P.-T. Liu and M.-C. Wu, *Nanoscale Res. Lett.*, 2014, **9**, 331.
26 Y.-C. Wang, B.-Y. Lin, P.-T. Liu and H.-P. D. Shieh, *Opt. Express*, 2014, **22**, A13.
27 L. C. Olsen and S. N. Kundu, *IEEE Photovoltaic Spec. Conf.*, 2005, 487.